

A Quasi-Newton Approach to Nonsmooth Convex Optimization

Jin Yu

S.V.N. Vishwanathan

Simon Günter

Nic Schraudolph

*Canberra Research Laboratory,
NICTA, Locked Bag 8001,
Canberra ACT 2601, Australia*

*Research School of Information Sciences and Engineering,
Australian National University,
Canberra ACT 0200, Australia*

JIN.YU@ANU.EDU.AU

SVN.VISHWANATHAN@NICTA.COM.AU

GUENTER_SIMON@HOTMAIL.COM

NIC@SCHRAUDOLPH.ORG

Editor: U.N.Known

Abstract

We extend the well-known BFGS quasi-Newton method and its limited-memory variant (LBFGS) to the optimization of nonsmooth convex objectives. This is done in a rigorous fashion by generalizing three components of BFGS to subdifferentials: The local quadratic model, the identification of a descent direction, and the Wolfe line search conditions. We apply the resulting subLBFGS algorithm to L_2 -regularized risk minimization with binary hinge loss, and its direction-finding component to L_1 -regularized risk minimization with logistic loss. In both settings our generic algorithms perform comparable to or better than their counterparts in specialized state-of-the-art solvers.

1. Introduction

The (L)BFGS quasi-Newton method (Nocedal and Wright, 1999) is widely regarded as the workhorse of *smooth* nonlinear optimization due to its combination of computational efficiency with good asymptotic convergence. Given a smooth objective function $J : \mathbb{R}^d \rightarrow \mathbb{R}$ and a current iterate $\mathbf{w}_t \in \mathbb{R}^d$, BFGS forms a local quadratic model of J :

$$Q_t(\mathbf{p}) := J(\mathbf{w}_t) + \frac{1}{2} \mathbf{p}^\top \mathbf{B}_t^{-1} \mathbf{p} + \nabla J(\mathbf{w}_t)^\top \mathbf{p}, \quad (1)$$

where $\mathbf{B}_t \succ 0$ is a positive-definite *estimate* of the inverse Hessian of J . Minimizing $Q_t(\mathbf{p})$ gives the quasi-Newton direction

$$\mathbf{p}_t := -\mathbf{B}_t \nabla J(\mathbf{w}_t), \quad (2)$$

which is used for the parameter update:

$$\mathbf{w}_{t+1} = \mathbf{w}_t + \eta_t \mathbf{p}_t. \quad (3)$$

The step size $\eta_t \in \mathbb{R}_+$ is normally determined by a line search obeying the Wolfe conditions:

$$\begin{aligned} J(\mathbf{w}_{t+1}) &\leq J(\mathbf{w}_t) + c_1 \eta_t \nabla J(\mathbf{w}_t)^\top \mathbf{p}_t \text{ and} \\ \nabla J(\mathbf{w}_{t+1})^\top \mathbf{p}_t &\geq c_2 \nabla J(\mathbf{w}_t)^\top \mathbf{p}_t, \end{aligned} \quad (4)$$

with $0 < c_1 < c_2 < 1$. The matrix \mathbf{B}_t is then modified via the incremental rank-two update

$$\mathbf{B}_{t+1} = (\mathbf{I} - \varrho_t \mathbf{s}_t \mathbf{y}_t^\top) \mathbf{B}_t (\mathbf{I} - \varrho_t \mathbf{y}_t \mathbf{s}_t^\top) + \varrho_t \mathbf{s}_t \mathbf{s}_t^\top, \quad (5)$$

where $\mathbf{s}_t := \mathbf{w}_{t+1} - \mathbf{w}_t$ and $\mathbf{y}_t := \nabla J(\mathbf{w}_{t+1}) - \nabla J(\mathbf{w}_t)$ denote the most recent step along the optimization trajectory in parameter and gradient space, respectively, and $\varrho_t := (\mathbf{y}_t^\top \mathbf{s}_t)^{-1}$. Given a descent direction \mathbf{p}_t , the Wolfe conditions ensure that $(\forall t) \mathbf{s}_t^\top \mathbf{y}_t > 0$ and hence $\mathbf{B}_0 \succ 0 \implies (\forall t) \mathbf{B}_t \succ 0$.

Limited-memory BFGS (LBFGS) is a variant of BFGS designed for solving large-scale optimization problems where the $O(d^2)$ cost of storing and updating \mathbf{B}_t would be prohibitively expensive. LBFGS approximates the quasi-Newton direction directly from the last m pairs of \mathbf{s}_t and \mathbf{y}_t via a matrix-free approach. This reduces cost to $O(md)$ space and time per iteration, with m freely chosen (Nocedal and Wright, 1999).

Smoothness of the objective function is essential for standard (L)BFGS because both the local quadratic model (1) and the Wolfe conditions (4) require the existence of the gradient ∇J at every point. Even though nonsmooth convex functions are differentiable everywhere except on a set of (Lebesgue) measure zero (Hiriart-Urruty and Lemaréchal, 1993), in practice (L)BFGS often fails to converge on such problems (Lukšan and Vlček, 1999; Haarala, 2004). Various subgradient-based approaches, such as subgradient descent (Nedich and Bertsekas, 2000) or bundle methods (Teo et al., 2007), are therefore preferred.

Although a convex function might not be differentiable everywhere, a subgradient always exists. Let \mathbf{w} be a point where a convex function J is finite. Then a subgradient is the normal vector of any tangential supporting hyperplane of J at \mathbf{w} . Formally, \mathbf{g} is called a subgradient of J at \mathbf{w} if and only if

$$J(\mathbf{w}') \geq J(\mathbf{w}) + (\mathbf{w}' - \mathbf{w})^\top \mathbf{g} \quad \forall \mathbf{w}'. \quad (6)$$

The set of all subgradients at a point is called the subdifferential, and is denoted by $\partial J(\mathbf{w})$. If this set is not empty then J is said to be *subdifferentiable at \mathbf{w}* . If it contains exactly one element, *i.e.*, $\partial J(\mathbf{w}) = \{\nabla J(\mathbf{w})\}$, then J is *differentiable at \mathbf{w}* .

In this paper we systematically modify the standard (L)BFGS algorithm so as to make it amenable to subgradients. This results in sub(L)BFGS, a new subgradient quasi-Newton method which is applicable to a wide variety of nonsmooth convex optimization problems encountered in machine learning.

In the next section we describe our new algorithm generically, before we discuss its application to the task of L_2 -regularized risk minimization with hinge loss in Section 3. Section 4 compares and contrasts our work with other recent efforts in this area. Encouraging experimental results are reported in Section 5. Finally, we conclude with an outlook and discussion in Section 6.

Algorithm 1 SUBBFGS

```

1: Initialize  $t := 0$ ,  $\mathbf{w}_0 = \mathbf{0}$ , and  $\mathbf{B}_0 = \mathbf{I}$ ;
2: Compute (sub)gradient  $\mathbf{g}_0 \in \partial J(\mathbf{w}_0)$ ;
3: while not converged do
4:    $\mathbf{p}_t = \text{descentDirection}(\mathbf{g}_t, \epsilon, k_{\max})$ ; (Algorithm 2)
5:   if  $\mathbf{p}_t = \text{failure}$  then
6:     Return  $\mathbf{w}_t$ ;
7:   end if
8:   Find  $\eta_t$  that obeys (14); (e.g. Algorithm 3)
9:    $\mathbf{s}_t = \eta_t \mathbf{p}_t$ ;
10:   $\mathbf{w}_{t+1} = \mathbf{w}_t + \mathbf{s}_t$ ;
11:  Compute (sub)gradient  $\mathbf{g}_{t+1} \in \partial J(\mathbf{w}_{t+1})$ ;
12:   $\mathbf{y}_t = \mathbf{g}_{t+1} - \mathbf{g}_t$ ;
13:  Update  $\mathbf{B}_{t+1}$  via (5);
14:   $t := t + 1$ ;
15: end while

```

2. BFGS Subgradient Method

We modify the standard BFGS algorithm to derive our new algorithm (subBFGS, Algorithm 1) for nonsmooth convex optimization. These modifications can be grouped into three areas, which we shall elaborate on in turn: generalizing the local quadratic model, finding a descent direction, and finding a step size that obeys a subgradient reformulation of the Wolfe conditions.

2.1 Generalizing the Local Quadratic Model

Recall that BFGS assumes the objective function J is differentiable everywhere, so that at the current iterate \mathbf{w}_t we can construct a local quadratic model (1) of $J(\mathbf{w}_t)$. For a nonsmooth objective function, such a model becomes ambiguous at non-differentiable points (Figure 1). To resolve the ambiguity, we could simply replace the gradient $\nabla J(\mathbf{w}_t)$ in (1) with some subgradient, $\mathbf{g}_t \in \partial J(\mathbf{w}_t)$. However, as will be discussed later, the resulting quasi-Newton direction $\mathbf{p}_t := -\mathbf{B}_t \mathbf{g}_t$ is *not* necessarily a descent direction. To address this fundamental modeling problem, we first generalize the local quadratic model as follows:

$$\begin{aligned}
Q_t(\mathbf{p}) &:= J(\mathbf{w}_t) + M_t(\mathbf{p}), \quad \text{where} \\
M_t(\mathbf{p}) &:= \frac{1}{2} \mathbf{p}^\top \mathbf{B}_t^{-1} \mathbf{p} + \sup_{\mathbf{g} \in \partial J(\mathbf{w}_t)} \mathbf{g}^\top \mathbf{p}.
\end{aligned} \tag{7}$$

Note that where J is differentiable, (7) reduces to the familiar BFGS quadratic model (1). At non-differentiable points, however, the model is no longer quadratic, as the supremum may be attained at different elements of $\partial J(\mathbf{w}_t)$ for different directions \mathbf{p} . Instead it can be viewed as the *tightest* pseudo-quadratic fit to J at \mathbf{w}_t (Figure 1).

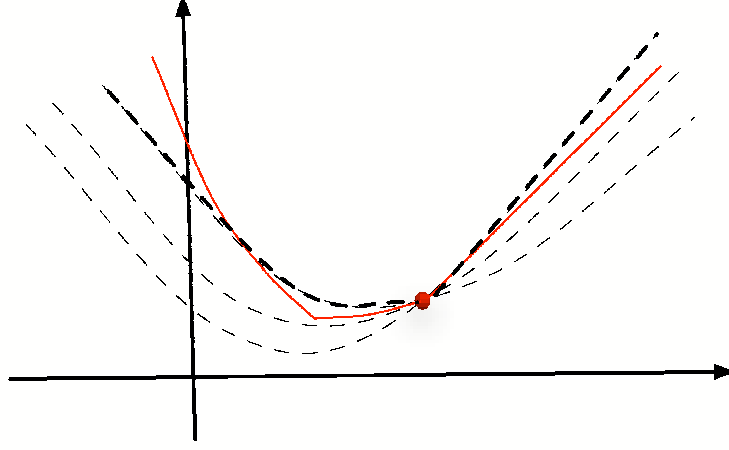


Figure 1: Possible quadratic models (dashed) at a subdifferentiable point (solid disk) versus tightest pseudo-quadratic approximation (7) (bold dashes) to the objective function (solid line).

Ideally, we would like to minimize $Q_t(\mathbf{p})$, or equivalently $M_t(\mathbf{p})$, in (7) to obtain the best search direction,

$$\mathbf{p}^* := \underset{\mathbf{p} \in \mathbb{R}^d}{\operatorname{arginf}} M_t(\mathbf{p}). \quad (8)$$

This is generally intractable due to the presence of a supremum over the entire subdifferential set $\partial J(\mathbf{w}_t)$. In many machine learning problems, however, the set $\partial J(\mathbf{w}_t)$ has some special structure that simplifies calculation of the supremum in (7). In what follows, we develop an iteration that is guaranteed to find a quasi-Newton descent direction, assuming an oracle that supplies $\operatorname{argsup}_{\mathbf{g} \in \partial J(\mathbf{w}_t)} \mathbf{g}^\top \mathbf{p}$ for a given direction $\mathbf{p} \in \mathbb{R}^d$. In Section 3.1 we provide an efficient implementation of such an oracle for L_2 -regularized risk minimization with the hinge loss.

2.2 Finding a Descent Direction

A direction \mathbf{p}_t is a descent direction if and only if $\mathbf{g}^\top \mathbf{p}_t < 0 \ \forall \mathbf{g} \in \partial J(\mathbf{w}_t)$ (Belloni, 2005), or equivalently

$$\sup_{\mathbf{g} \in \partial J(\mathbf{w}_t)} \mathbf{g}^\top \mathbf{p}_t < 0. \quad (9)$$

In particular, for a smooth convex function the quasi-Newton direction (2) is always a descent direction because $\nabla J(\mathbf{w}_t)^\top \mathbf{p}_t = -\nabla J(\mathbf{w}_t)^\top \mathbf{B}_t \nabla J(\mathbf{w}_t) < 0$ holds due to the positivity of \mathbf{B}_t .

For nonsmooth functions, however, the quasi-Newton direction $\mathbf{p}_t := -\mathbf{B}_t \mathbf{g}_t$ for a given $\mathbf{g}_t \in \partial J(\mathbf{w}_t)$ may not fulfill the descent condition (9), making it impossible to find a step that

Algorithm 2 $\mathbf{p}_t = \text{descentDirection}(\mathbf{g}^1, \epsilon, k_{\max})$

```

1: input (sub)gradient  $\mathbf{g}^1 \in \partial J(\mathbf{w}_t)$ , tolerance  $\epsilon \in \mathbb{R}_+$ , and maximal number of iteration  $k_{\max}$ ;
2: output descent direction  $\mathbf{p}_t$ ;
3: Initialize  $i = 1$ ,  $\bar{\mathbf{g}}^1 = \mathbf{g}^1$ ,  $\mathbf{p}^1 = -\mathbf{B}_t \mathbf{g}^1$ ;
4:  $\mathbf{g}^2 = \text{argsup}_{\mathbf{g} \in \partial J(\mathbf{w}_t)} \mathbf{g}^\top \mathbf{p}^1$ ;
5: Calculate  $\epsilon^1$  (13);
6: while  $(\mathbf{g}^{i+1})^\top \mathbf{p}^i > 0$  or  $\epsilon^i > \epsilon$  and  $i < k_{\max}$  do
7:    $\mu^* := \min \left( 1, \frac{(\mathbf{g}^{i+1} - \bar{\mathbf{g}}^i)^\top \mathbf{p}^i}{(\mathbf{g}^{i+1} - \bar{\mathbf{g}}^i)^\top \mathbf{B}_t (\mathbf{g}^{i+1} - \bar{\mathbf{g}}^i)} \right)$  (54)
8:    $\bar{\mathbf{g}}^{i+1} = (1 - \mu^*) \bar{\mathbf{g}}^i + \mu^* \mathbf{g}^{i+1}$ ;
9:    $\mathbf{p}^{i+1} = (1 - \mu^*) \mathbf{p}^i - \mu^* \mathbf{B}_t \mathbf{g}^{i+1}$ ;
10:   $\mathbf{g}^{i+2} = \text{argsup}_{\mathbf{g} \in \partial J(\mathbf{w}_t)} \mathbf{g}^\top \mathbf{p}^{i+1}$ ;
11:  Calculate  $\epsilon^{i+1}$  (13);
12:   $i := i + 1$ ;
13: end while
14: if  $\mathbf{g}^{i+1})^\top \mathbf{p}^i > 0$  then
15:   return failure;
16: else
17:   return  $\text{argmin}_{j \leq i} M_t(\mathbf{p}^j)$ .
18: end if

```

obeys (4), thus causing a failure of the line search. We now present an iterative approach to find a quasi-Newton *descent* direction.

Inspired by bundle methods (Teo et al., 2007), we build the following convex lower bound on $M_t(\mathbf{p})$:

$$M_t^i(\mathbf{p}) := \frac{1}{2} \mathbf{p}^\top \mathbf{B}_t^{-1} \mathbf{p} + \sup_{j \leq i} \mathbf{g}^j \mathbf{p}, \quad i, j \in \mathbb{N}. \quad (10)$$

Given a $\mathbf{p}^i \in \mathbb{R}^d$ the lower bound (10) is successively tightened by computing

$$\mathbf{g}^{i+1} := \text{argsup}_{\mathbf{g} \in \partial J(\mathbf{w}_t)} \mathbf{g}^\top \mathbf{p}^i, \quad (11)$$

such that $M_t^i(\mathbf{p}) \leq M_t^{i+1}(\mathbf{p}) \leq M_t(\mathbf{p}) \quad \forall \mathbf{p} \in \mathbb{R}^d$. Here we set $\mathbf{g}^1 \in \partial J(\mathbf{w}_t)$, and assume that \mathbf{g}^{i+1} is provided by an oracle. To solve $\inf_{\mathbf{p} \in \mathbb{R}^d} M_t^i(\mathbf{p})$, we rewrite it as a constrained optimization problem:

$$\inf_{\mathbf{p}, \xi} \frac{1}{2} \mathbf{p}^\top \mathbf{B}_t^{-1} \mathbf{p} + \xi, \quad \text{s.t.} \quad \mathbf{g}^j \mathbf{p} \leq \xi \quad \forall j \leq i. \quad (12)$$

This problem can be solved exactly via quadratic programming (QP), but doing so may incur substantial computational expense. Instead we adopt an alternate approach (Algorithm 2) which *does not* solve $\inf_{\mathbf{p} \in \mathbb{R}^d} M_t^i(\mathbf{p})$ to optimality. The key idea is to write the proposed descent direction at iteration $i + 1$ as a convex combination of \mathbf{p}^i and $-\mathbf{B}_t \mathbf{g}^{i+1}$. The

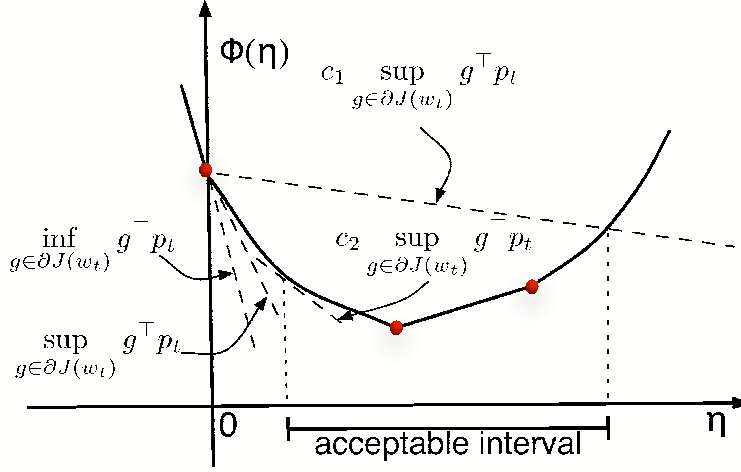


Figure 2: Geometric interpretation of the subgradient Wolfe conditions. Solid disks are subdifferentiable points. The slopes of dashed lines are indicated.

optimal combination coefficient μ^* can be computed exactly (Step 5 of Algorithm 2) using an argument based on maximizing dual progress. Finally, to derive an implementable stopping criterion, we define

$$\epsilon^i := \min_{j \leq i} \mathbf{p}^j \top \mathbf{g}^{j+1} - \frac{1}{2} (\mathbf{p}^j \top \bar{\mathbf{g}}^j + \mathbf{p}^i \top \bar{\mathbf{g}}^i), \quad (13)$$

where $\bar{\mathbf{g}}^i$ is an aggregated subgradient (Step 6 of Algorithm 2) which lies in the convex hull of $\mathbf{g}^j \in \partial J(\mathbf{w}_t) \forall j \leq i$. ϵ^i is monotonically decreasing, and upper bounds the distance from the optimal value of the dual of $M_t(\mathbf{p})$. This guides us to design a practical stopping criteria (Step 4 of Algorithm 2) for our direction-finding procedure. Details can be found in Appendix A, where we also prove that Algorithm 2 converges to the optimal dual objective value with precision ϵ at an $O(1/\epsilon)$ rate.

2.3 Subgradient Line Search

Given the current iterate \mathbf{w}_t and a search direction \mathbf{p}_t , the task of a line search is to find a step size $\eta \in \mathbb{R}_+$ which decreases the objective function along the line $\mathbf{w}_t + \eta \mathbf{p}_t$, i.e., $J(\mathbf{w}_t + \eta \mathbf{p}_t) =: \Phi(\eta)$. The Wolfe conditions (4) are used in line search routines to enforce a sufficient decrease in the objective value, and to exclude unnecessarily small step sizes (Nocedal and Wright, 1999). However, the original Wolfe conditions require the objective function to be smooth. To extend them to nonsmooth convex problems, we propose the

following subgradient reformulation:

$$\begin{aligned} J(\mathbf{w}_{t+1}) &\leq J(\mathbf{w}_t) + c_1 \eta_t \sup_{\mathbf{g} \in \partial J(\mathbf{w}_t)} \mathbf{g}^\top \mathbf{p}_t, \text{ and} \\ \sup_{\mathbf{g}' \in \partial J(\mathbf{w}_{t+1})} \mathbf{g}'^\top \mathbf{p}_t &\geq c_2 \sup_{\mathbf{g} \in \partial J(\mathbf{w}_t)} \mathbf{g}^\top \mathbf{p}_t, \end{aligned} \quad (14)$$

where $0 < c_1 < c_2 < 1$. Figure 2 illustrates how these conditions enforce acceptance of non-trivial step sizes that decrease the objective value. In Appendix B we formally show that for any given descent direction we can always find a positive step size that satisfies (14).

2.4 Limited-Memory subBFGS (subLBFGS)

It is straightforward to implement an LBFGS variant of our subBFGS algorithm: We simply modify Algorithms 1 and 2 to compute all products of \mathbf{B}_t with a vector by means of the standard LBFGS matrix-free scheme (Nocedal and Wright, 1999).

3. sub(L)BFGS Implementation for L_2 -Regularized Risk Minimization

Many machine learning algorithms can be viewed as minimizing a convex regularized risk:

$$J(\mathbf{w}) := \frac{c}{2} \|\mathbf{w}\|^2 + \frac{1}{n} \sum_{i=1}^n l(\mathbf{w}^\top \mathbf{x}_i, z_i), \quad (15)$$

where $\mathbf{x}_i \in \mathcal{X} \subseteq \mathbb{R}^d$ are the training instances, $z_i \in \mathcal{Z} \subseteq \mathbb{R}$ the corresponding labels, and l , the loss, is a non-negative convex function of \mathbf{w} which measures the discrepancy between z_i and the predictions arising from \mathbf{w} via $\mathbf{w}^\top \mathbf{x}_i$. A loss function commonly used for binary classification is the hinge loss:

$$l(\mathbf{w}^\top \mathbf{x}, z) := \max(0, 1 - z \mathbf{w}^\top \mathbf{x}), \quad (16)$$

where $z \in \{\pm 1\}$. It is easy to see that regularized risk minimization with the binary hinge loss is a convex but nonsmooth optimization problem. In this section we show how sub(L)BFGS (Algorithm 1) can be applied to this problem.

Differentiating (15) after plugging in (16) yields:

$$\begin{aligned} \partial J(\mathbf{w}) &= c\mathbf{w} - \frac{1}{n} \sum_{i=1}^n \beta_i z_i \mathbf{x}_i = \bar{\mathbf{w}} - \frac{1}{n} \sum_{i \in \mathcal{M}} \beta_i z_i \mathbf{x}_i, \\ \text{where } \bar{\mathbf{w}} &:= c\mathbf{w} - \frac{1}{n} \sum_{i \in \mathcal{E}} z_i \mathbf{x}_i \text{ and} \end{aligned} \quad (17)$$

$$\beta_i := \begin{cases} 1 & \text{if } i \in \mathcal{E}, \quad \mathcal{E} := \{i : 1 - z_i \mathbf{w}^\top \mathbf{x}_i > 0\}, \\ [0, 1] & \text{if } i \in \mathcal{M}, \quad \mathcal{M} := \{i : 1 - z_i \mathbf{w}^\top \mathbf{x}_i = 0\}, \\ 0 & \text{if } i \in \mathcal{W}, \quad \mathcal{W} := \{i : 1 - z_i \mathbf{w}^\top \mathbf{x}_i < 0\}. \end{cases}$$

\mathcal{E} , \mathcal{M} , and \mathcal{W} denote the set of points which are in error, on the margin, and well-classified, respectively.

3.1 Realizing the Direction-Finding Method

Recall that in order to apply our sub(L)BFGS algorithm to a problem one needs an oracle that provides $\operatorname{argsup}_{\mathbf{g} \in \partial J(\mathbf{w}_t)} \mathbf{g}^\top \mathbf{p}$ for a given direction \mathbf{p} . For L_2 -regularized risk minimization with binary hinge loss we can implement such an oracle at computational cost linear in the number $|\mathcal{M}_t|$ of current marginal points. (Normally $|\mathcal{M}_t| \ll n$.) Towards this end we use (17) to obtain

$$\sup_{\mathbf{g} \in \partial J(\mathbf{w}_t)} \mathbf{g}^\top \mathbf{p} = \sup_{\beta_i, i \in \mathcal{M}_t} \left(\bar{\mathbf{w}}_t - \frac{1}{n} \sum_{i \in \mathcal{M}_t} \beta_i z_i \mathbf{x}_i \right)^\top \mathbf{p} = \bar{\mathbf{w}}_t^\top \mathbf{p} - \frac{1}{n} \sum_{i \in \mathcal{M}_t} \sup_{\beta_i \in [0,1]} (\beta_i z_i \mathbf{x}_i^\top \mathbf{p}). \quad (18)$$

Since for a given \mathbf{p} the first term of the right-hand side of (18) is a constant, the supremum is attained when we set $\beta_i \forall i \in \mathcal{M}_t$ via the following strategy:

$$\beta_i := \begin{cases} 0 & \text{if } z_i \mathbf{x}_i^\top \mathbf{p}_t \geq 0, \\ 1 & \text{if } z_i \mathbf{x}_i^\top \mathbf{p}_t < 0. \end{cases} \quad (19)$$

3.2 Implementing the Line Search

We first show that the one-dimensional convex function obtained by restricting (15) to a line can be evaluated efficiently. To see this rewrite the objective as

$$J(\mathbf{w}) := \frac{c}{2} \|\mathbf{w}\|^2 + \frac{1}{n} \mathbf{1}^\top \max(\mathbf{0}, \mathbf{1} - \mathbf{z} \cdot (\mathbf{X}\mathbf{w})), \quad (20)$$

where $\mathbf{0}$ and $\mathbf{1}$ are column vectors of zeros and ones, respectively, \cdot denotes the Hadamard (component-wise) product, and $\mathbf{z} \in \mathbb{R}^n$ collects correct labels corresponding to each row of data in $\mathbf{X} := [\mathbf{x}_1, \mathbf{x}_2, \dots, \mathbf{x}_n]^\top \in \mathbb{R}^{n \times d}$. Given a search direction \mathbf{p}_t at an iterate \mathbf{w}_t this allows us to write

$$\Phi(\eta) := J(\mathbf{w}_t + \eta \mathbf{p}_t) = \frac{c}{2} \|\mathbf{w}_t\|^2 + c\eta \mathbf{w}_t^\top \mathbf{p}_t + \frac{c\eta^2}{2} \|\mathbf{p}_t\|^2 + \frac{1}{n} \boldsymbol{\delta}_\eta^\top (\mathbf{1} - (\mathbf{f} + \eta \Delta \mathbf{f})), \quad (21)$$

where $\mathbf{f} := \mathbf{z} \cdot (\mathbf{X}\mathbf{w}_t)$, $\Delta \mathbf{f} := \mathbf{z} \cdot (\mathbf{X}\mathbf{p}_t)$, and for $1 \leq i \leq n$

$$\delta_\eta(i) := \begin{cases} 1 & \text{if } \mathbf{f}(i) + \eta \Delta \mathbf{f}(i) < 1, \\ [0, 1] & \text{if } \mathbf{f}(i) + \eta \Delta \mathbf{f}(i) = 1, \\ 0 & \text{if } \mathbf{f}(i) + \eta \Delta \mathbf{f}(i) > 1. \end{cases} \quad (22)$$

We cache \mathbf{f} and $\Delta \mathbf{f}$, expending $O(nd)$ computational effort. We also cache $\frac{c}{2} \|\mathbf{w}_t\|^2$, $c\mathbf{w}_t^\top \mathbf{p}_t$, and $\frac{c}{2} \|\mathbf{p}_t\|^2$, each of which requires $O(n)$ work. Computing $\Phi(\eta)$ from this information requires the evaluation of $\boldsymbol{\delta}_\eta$ and $\boldsymbol{\delta}_\eta^\top (\mathbf{1} - (\mathbf{f} + \eta \Delta \mathbf{f}))$, both of which can be calculated with $O(n)$ effort. All other terms in (21) can be computed in constant time, thus reducing the overall complexity of evaluating $\Phi(\eta)$ to $O(n)$. We are now in a position to introduce an exact line search which takes advantage of this scheme.

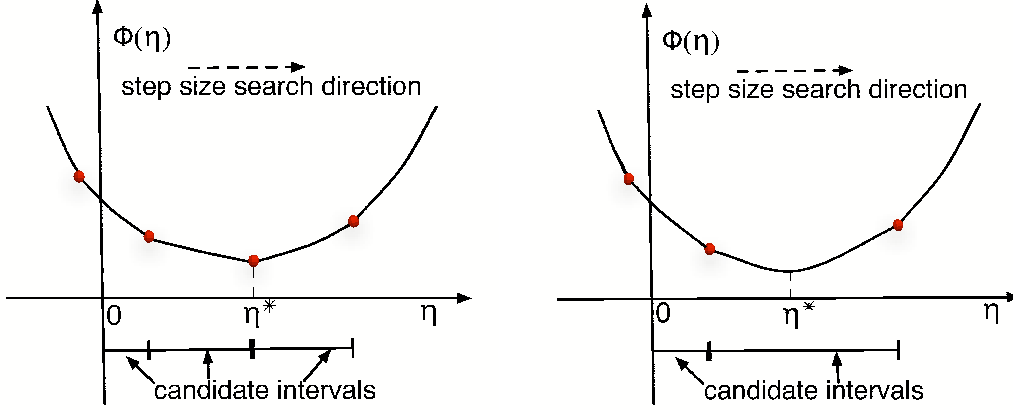


Figure 3: Nonsmooth quadratic function Φ of step size η . Solid disks are subdifferentiable points. The optimal η^* can be a subdifferentiable point (left), or lie inbetween two subdifferentiable points (right).

3.2.1 EXACT LINE SEARCH

Differentiating (21) with respect to η and setting the gradient to 0 shows that $\eta^* := \operatorname{argmin}_{\eta} \Phi(\eta)$ satisfies

$$\eta^* = \frac{\frac{1}{n} \delta_{\eta^*}^\top \Delta \mathbf{f} - c \mathbf{w}_t^\top \mathbf{p}_t}{c \|\mathbf{p}_t\|^2}.$$

It is easy to verify that $\Phi(\eta)$ is piecewise quadratic (Figure 3). It is differentiable everywhere except at $\eta = (1 - \mathbf{f}(i)) / \Delta \mathbf{f}(i)$, where it becomes subdifferentiable. At all these points an element of the indicator vector δ_η (22) changes from 0 to 1 or vice versa, implying that δ_η remains constant in the interval between two subdifferentiable points, say (η_a, η_b) .

This motivates the following line search strategy: For each candidate interval (η_a, η_b) compute the candidate step size

$$\eta_{\text{trial}}^* = \frac{\frac{1}{n} \delta_{\eta'}^\top \Delta \mathbf{f} - c \mathbf{w}_t^\top \mathbf{p}_t}{c \|\mathbf{p}_t\|^2}, \quad \text{where } \eta' \in (\eta_a, \eta_b),$$

and accept it if $\eta_{\text{trial}}^* \in [\eta_a, \eta_b]$, otherwise accept η_a if $0 \in \partial \Phi(\eta_a)$. The full implementation is detailed in Algorithm 3.

4. Related Work

Lukšan and Vlček (1999) propose an extension of BFGS to nonsmooth convex problems. Their algorithm samples gradients around non-differentiable points in order to obtain a descent direction. In many machine learning problems evaluating the objective function and its gradient is very expensive. Therefore, our direction finding algorithm (Algorithm 2)

Algorithm 3 $\eta = \text{linesearch}(\mathbf{w}_t, \mathbf{p}_t, c, \mathbf{f}, \Delta \mathbf{f})$

```

1: input  $\mathbf{w}_t, \mathbf{p}_t, c, \mathbf{f}$ , and  $\Delta \mathbf{f}$  as in (21);
2: output Step size  $\eta$ ;
3:  $b = c \mathbf{w}_t^\top \mathbf{p}_t, h = c \|\mathbf{p}_t\|^2$ , and  $n = \text{length}(\mathbf{f})$ ;
4: Compute subdifferentiable points,  $\boldsymbol{\alpha} := \frac{1-\mathbf{f}}{\Delta \mathbf{f}}$ ;
5:  $\boldsymbol{\alpha}^+ = \text{QuickSort}(\boldsymbol{\alpha}(\boldsymbol{\alpha} > 0))$ ;
6:  $\text{index} = \text{find}(\boldsymbol{\alpha} = \boldsymbol{\alpha}^+)$ ;
7:  $\boldsymbol{\alpha} := [0; \boldsymbol{\alpha}^+]$ ;
8: Initialize  $\eta \in (\boldsymbol{\alpha}(1), \boldsymbol{\alpha}(2))$ ;
9: for  $i := 1$  to  $n$  do
10:    $\delta(i) := \begin{cases} 1 & \text{if } \mathbf{f}(i) + \eta \Delta \mathbf{f}(i) < 1; \\ 0 & \text{otherwise;} \end{cases}$ 
11: end for
12: Set  $j := 2$  and  $\varrho := \delta^\top \Delta \mathbf{f} / n$ ;
13: while  $j \leq \text{length}(\boldsymbol{\alpha})$  do
14:   Compute exact step size,  $\eta := (\varrho - b) / h$ ;
15:   if  $\eta \in [\boldsymbol{\alpha}(j-1), \boldsymbol{\alpha}(j)]$  then
16:     Return  $\eta$ ;
17:   else if  $\eta < \boldsymbol{\alpha}(j-1)$  then
18:     Return  $\eta := \boldsymbol{\alpha}(j-1)$ ;
19:   else
20:     repeat
21:       Set  $i = \text{index}(j)$ ;
22:        $\delta(i) := 1 - \delta(i)$ ;
23:        $\varrho := \begin{cases} \varrho + \Delta \mathbf{f}(i) / n & \text{if } \delta(i) = 1, \\ \varrho - \Delta \mathbf{f}(i) / n & \text{otherwise;} \end{cases}$ 
24:        $j := j + 1$ ;
25:     until  $\boldsymbol{\alpha}(j) \neq \boldsymbol{\alpha}(j-1)$ 
26:   end if
27: end while

```

repeatedly samples subgradients from the set $\partial J(\mathbf{w})$ via the oracle, which is computationally more efficient.

Recently, Andrew and Gao (2007) introduced a variant of nonsmooth BFGS, Orthant-Wise Limited-memory Quasi-Newton (OWL-QN) algorithm, suitable for optimizing L_1 -regularized log-linear models:

$$J(\mathbf{w}) := c \|\mathbf{w}\|_1 + \frac{1}{n} \sum_{i=1}^n \ln(1 + \exp(-z_i \mathbf{w}^\top \mathbf{x}_i)), \quad (23)$$

where the logistic loss is smooth, but the regularizer is nonsmooth since it is only subdifferentiable whenever \mathbf{w} has zero elements. From the viewpoint of an optimization algorithm this objective function is very similar to the L_2 -regularized hinge loss problem; the direction finding method and the line search that we discussed in Sections 3.1 and 3.2, respectively can be applied to this problem with slight modifications.

Table 1: Four datasets.

Datasets	Tr./Te.data	Dim.	Density
Coverttype	522911/58101	54	22.22%
CCAT	781265/23149	47236	0.16%
Astro	29882/32487	99757	0.077%
MNIST	60000/10000	780	19.22%

Table 2: Regularization constants c , direction-finding convergence criterion ϵ , and the overall number k of direction-finding iterations for L_1 -regularized logistic loss and L_2 -regularized hinge loss minimization tasks, respectively.

Datasets	c_{L_1}	ϵ_{L_1}	k_{L_1}	$k_{L_1\text{rand}}$	c_{L_2}	ϵ_{L_2}	k_{L_2}
Coverttype	10^{-6}	10^{-5}	0	0	10^{-6}	10^{-8}	44
CCAT	10^{-6}	10^{-5}	356	467	10^{-4}	10^{-8}	66
Astro	10^{-5}	10^{-3}	1668	2840	$5 \cdot 10^{-5}$	10^{-8}	17
MNIST	10^{-4}	10^{-5}	60	102	$1.4286 \cdot 10^{-6}$	10^{-8}	244

OWL-QN is based on the observation that the L_1 regularizer is linear within any given orthant. Therefore, it maintains an approximation \mathbf{B}_{ow} to the inverse Hessian of the logistic loss, and uses an efficient scheme to select orthants for optimization. In fact, its success greatly depends on its direction-finding subroutine, which demands a specially chosen subgradient \mathbf{g}_{ow} (Equation 4 in Andrew and Gao (2007)) to produce the quasi-Newton direction, $\mathbf{p}_{\text{ow}} = \pi(-\mathbf{B}_{\text{ow}}\mathbf{g}_{\text{ow}}, -\mathbf{g}_{\text{ow}})$, where the projection π returns a search direction by setting the i^{th} element of $-\mathbf{B}_{\text{ow}}\mathbf{g}_{\text{ow}}$ to zero whenever $(\mathbf{B}_{\text{ow}}\mathbf{g}_{\text{ow}})(i) \times \mathbf{g}_{\text{ow}}(i) < 0$. As shown in Section 5, the direction-finding subroutine of OWL-QN can be replaced by Algorithm 2, which in turn makes the algorithm more robust to the choice of subgradients.

Many optimization techniques use past gradients to build a model of the objective function. Bundle method solvers like BMRM (Teo et al., 2007) and SVMStruct (Joachims, 2006) use them to lower-bound the objective by a piecewise linear function which is minimized to obtain the next iterate. This fundamentally differs from the BFGS approach of using past gradients to approximate the (inverse) Hessian, hence building a quadratic model of the objective function.

Vojtěch and Sönnenburg (2007) speed up the convergence of a bundle method solver for the L_2 -regularized binary hinge loss. Their main idea is to perform a line search along the line connecting two successive iterates of a bundle method solver. Although developed independently, their line search algorithm is very reminiscent of the method we describe in Section 3.2.1.

5. Experiments

We now evaluate the performance of our algorithm, subLBFGS, and compare it to other state-of-the-art nonsmooth optimization methods on the L_2 -regularized hinge loss mini-

mization. A variant of OWL-QN that uses our direction-finding routine is applied to the L_1 -regularized logistic loss minimization and compared with the original.

Table 1 lists four datasets that were used in our experiments: Covertypes dataset ¹ of Blackard, Jock & Dean; CCAT from the Reuters RCV1 collection; ² Astro-physics dataset of abstracts of scientific papers from the Physics ArXiv (Joachims, 2006) and MNIST dataset of handwritten digits ³ with two classes: even and odd digits. We used subLBFGS with a buffer of size $m = 15$ throughout. Table 2 summarizes our parameter settings, and reports the overall number of direction-finding inner loops for all experiments. We followed the choices of Vojtěch and Sönnenburg (2007) for the L_2 regularization constants; for L_1 they were chosen from the set $10^{\{-6, -5, \dots, -1\}}$ to achieve the highest prediction rate on the test dataset.

Note that on convex problems such as these every convergent optimizer will reach the same solution; comparing generalisation performance is therefore pointless. We combined training and test datasets to evaluate the convergence of each algorithm in terms of the objective function value *vs.* CPU seconds. All experiments were carried out on a Linux machine with dual 2.8 GHz Xeon processors with 4GB RAM.

5.1 L_2 -Regularized Hinge Loss

For our first set of experiments, we applied subLBFGS together with our exact line search (Algorithm 3) to the task of L_2 -regularized hinge loss minimization. Our competing algorithms are the bundle method solver BMRM (Teo et al., 2007) and an optimized cutting plane algorithm, OCAS version 0.6.0 (Vojtěch and Sönnenburg, 2007), ⁴ both of which demonstrated strong results on the L_2 -regularized hinge loss minimization in their corresponding papers.

Figure 4 shows subLBFGS (solid) converges noticeably (up to 7 times) faster toward the neighbourhood of the optimum (less than 10^{-3} away from the optimum) than BMRM (dashed). As BMRM’s approximation to the objective function improves over the course of optimization, it gradually catches up with subLBFGS, though it is still outperformed by subLBFGS on 3 out of 4 datasets in terms of final convergence speed. The performance of subLBFGS and OCAS (dash-dotted) are very similar. OCAS converges slightly faster than subLBFGS on the Astro-physics dataset, while it is outperformed by subLBFGS on the MNIST dataset.

5.2 L_1 -Regularized Logistic Loss

To demonstrate the utility of our direction-finding routine (Algorithm 2) in its own right, we plugged it into the OWL-QN algorithm (Andrew and Gao, 2007) ⁵ as an alternative direction-finding method such that $\mathbf{p}_{\text{ow}} = \text{descentDirection}(\mathbf{g}_{\text{ow}}, \epsilon, k_{\text{max}})$, ⁶ and compared

1. <http://kdd.ics.uci.edu/databases/covertypes/covertypes.html>

2. <http://www.daviddlewis.com/resources/testcollections/rcv1>

3. <http://yann.lecun.com/exdb/mnist>

4. The source code of OCAS (version 0.6.0) was downloaded from <http://www.shogun-toolbox.org>.

5. The source code of OWL-QN (original release) was downloaded from <http://research.microsoft.com/research/downloads/Details/b1eb1016-1738-4bd5-83a9-370c9d498a03/Details>.

6. Note for the objective (23) it is trivial to construct an oracle that supplies $\text{argsup}_{\mathbf{g} \in \partial J(\mathbf{w}_t)} \mathbf{g}^\top \mathbf{p}$.

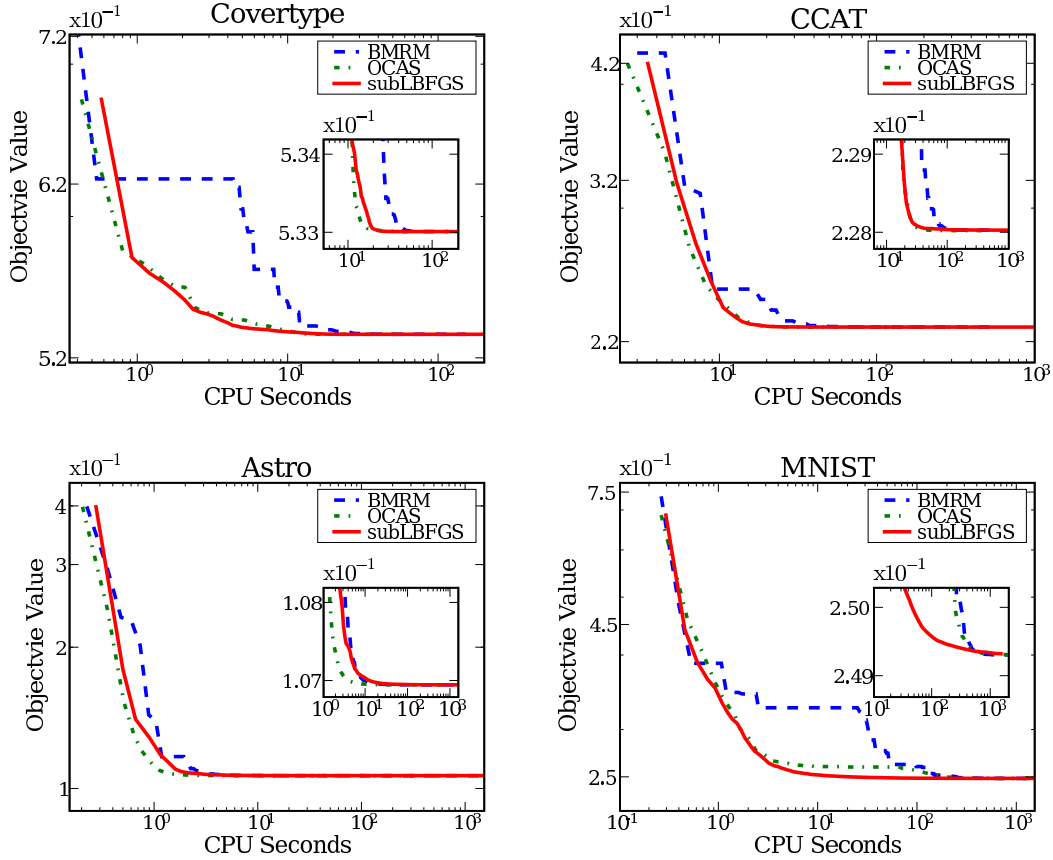


Figure 4: Objective function value *vs.* CPU seconds on L_2 -regularized hinge loss minimization tasks in log-log scale.

this variant (denoted by OWL-QN*) with the original on L_1 -regularized logistic loss minimization.

Using the stopping criteria suggested by Andrew and Gao (2007), we run experiments until the averaged relative change in the objective value over the previous 5 iterations falls below 10^{-5} . Figure 5 shows that there are only minor differences in convergence between the two algorithms.

To examine the sensitivity of the algorithms to the choice of subgradients, we also ran them with random subgradients (as opposed to the specially chosen subgradient \mathbf{g}_{ow} used in the previous set of experiments) fed to their corresponding direction-finding routines. OWL-QN relies heavily on its particular choice of subgradients, hence breaks down completely under these conditions: The only dataset where we could even plot its (poor) performance was Covertypes (dotted OWL-QN(2) line in Figure 5). Our direction-finding routine, by contrast, is self-correcting (Table 2 shows that in this case more direction-finding loops are executed, *i.e.*, $k_{L_1\text{rand}} \geq k_{L_1}$) and thus not affected by this manipulation: The curves for OWL-QN*(2) (plotted for Covertypes in Figure 5) lie almost on top of those for OWL-QN*.

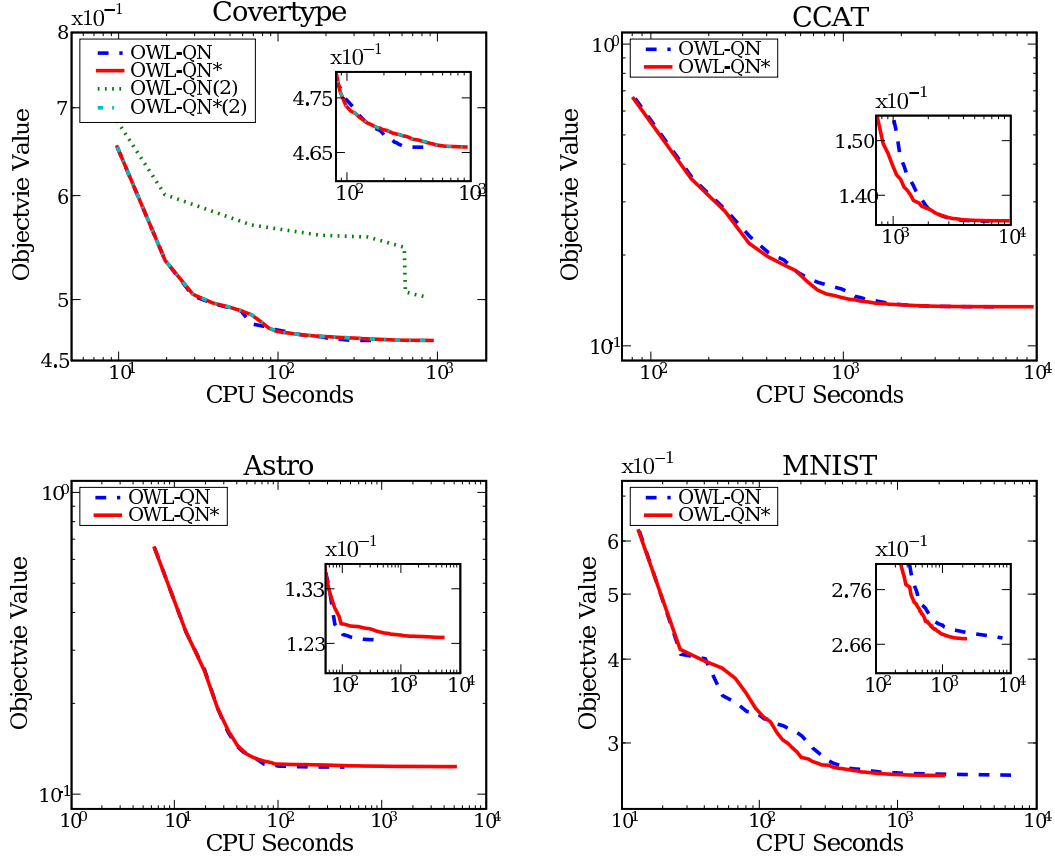


Figure 5: Objective value *vs.* CPU seconds on L_1 -regularized logistic loss minimization tasks in log-log scale.

This empirically confirms that as long as $\operatorname{argsup}_{\mathbf{g} \in \partial J(\mathbf{w}_t)} \mathbf{g}^\top \mathbf{p}$ is given, Algorithm 2 can indeed be used as a canned quasi-Newton direction-finding routine.

6. Outlook and Discussion

We proposed an extension of BFGS suitable for handling nonsmooth problems often encountered in the machine learning context. As our experiments show, our algorithms are versatile and applicable to many problems. At the same time their performance is comparable to if not better than that of their counterparts in custom-built solvers.

In some experiments we observe that subLBFGS initially makes rapid progress towards the solution but slows down closer to the optimum. We hypothesize that initially its quadratic model allows subLBFGS to make rapid progress, but closer to the optimum it is no longer an accurate model of an objective function dominated by the nonsmooth hinges. We are therefore contemplating hybrid solvers which seamlessly switch between sub(L)BFGS and bundle solvers.

In this paper we applied subLBFGS to L_2 -regularized risk minimization with binary hinge loss. It can also be extended to deal with generalizations of the hinge loss, *e.g.* multi-class, multi-category, and ordinal regression problems. This is part of our ongoing research.

Finally, to put our contributions in perspective, recall that we modified three aspects of the standard BFGS algorithm, namely the quadratic model (Section 2.1), the descent direction finding (Section 2.2), and the line search (Section 2.3). Each of these modifications is versatile enough to be used as a component in other nonsmooth optimization algorithms. This not only offers the promise of improving existing algorithms, but may also help clarify connections between them. We hope that this will focus attention on those core subroutines that need to be made more efficient in order to handle larger and larger datasets.

Acknowledgement

NICTA is funded by the Australian Government’s Backing Australia’s Ability and the Centre of Excellence programs. This work is also supported by the IST Program of the European Community, under the FP7 Network of Excellence, ICT-216886-NOE.

References

- N. Abe, J. Takeuchi, and M.K. Warmuth. Polynomial Learnability of Stochastic Rules with Respect to the KL-Divergence and Quadratic Distance. *IEICE Transactions on Information and Systems*, 84(3):299–316, 2001.
- Galen Andrew and Jianfeng Gao. Scalable training of l1-regularized log-linear models. In *Proc. Intl. Conf. Machine Learning*, pages 33–40, New York, NY, USA, 2007. ACM.
- Alexandre Belloni. Introduction to bundle methods. Technical report, Operation Research Center, M.I.T., 2005.
- Marjo Haarala. *Large-Scale Nonsmooth Optimization*. PhD thesis, University of Jyväskylä, 2004.
- J.B. Hiriart-Urruty and C. Lemaréchal. *Convex Analysis and Minimization Algorithms, I and II*. 305 and 306. Springer-Verlag, 1993.
- T. Joachims. Training linear SVMs in linear time. In *Proceedings of the ACM Conference on Knowledge Discovery and Data Mining (KDD)*. ACM, 2006.
- L. Lukšan and J. Vlček. Globally convergent variable metric method for convex nonsmooth unconstrained minimization. *Journal of Optimization Theory and Applications*, 102(3): 593–613, 1999.
- A. Nedich and D. P Bertsekas. Convergence rate of incremental subgradient algorithms. In S. Uryasev and P. M. Pardalos, editors, *Stochastic Optimization: Algorithms and Applications*, pages 263–304. Kluwer Academic Publishers, 2000.
- J. Nocedal and S. J. Wright. *Numerical Optimization*. Springer Series in Operations Research. Springer, 1999.

C.H. Teo, Q. Le, A.J. Smola, and S.V.N. Vishwanathan. A scalable modular convex solver for regularized risk minimization. In *Conference on Knowledge Discovery and Data Mining*, 2007.

F. Vojtěch and S. Sönnenburg. Optimized cutting plane algorithm for support vector machines. Technical Report 1, Fraunhofer Institute FIRST, December 2007. <http://publica.fraunhofer.de/documents/N-66225.html>.

Appendix A. Bundle Search for Descent Direction

Recall from Section 2.2 that at a subdifferential point \mathbf{w} our goal is to find a descent direction \mathbf{p}^* which minimizes the pseudo-quadratic model:⁷

$$M(\mathbf{p}) := \frac{1}{2}\mathbf{p}^\top \mathbf{B}^{-1}\mathbf{p} + \sup_{\mathbf{g} \in \partial J(\mathbf{w})} \mathbf{g}^\top \mathbf{p}. \quad (24)$$

However, this is generally intractable due to the presence of a supremum over the entire subdifferential $\partial J(\mathbf{w})$. Therefore, we propose a bundle-based descent direction finding procedure (Algorithm 2), which progressively approaches $M(\mathbf{p})$ from below via a series of convex functions: $M^1(\mathbf{p}), \dots, M^i(\mathbf{p})$, each taking the same form as $M(\mathbf{p})$, but where the supremum is defined over a countable subset of $\partial J(\mathbf{w})$. At step i our convex lower bound $M^i(\mathbf{p})$ takes the form

$$M^i(\mathbf{p}) := \frac{1}{2}\mathbf{p}^\top \mathbf{B}^{-1}\mathbf{p} + \sup_{\mathbf{g} \in V^i} \mathbf{g}^\top \mathbf{p}, \text{ where} \\ V^i := \{\mathbf{g}^j : j \leq i, i, j \in \mathbb{N}\} \subseteq \partial J(\mathbf{w}). \quad (25)$$

Given an iterate $\mathbf{p}^{j-1} \in \mathbb{R}^d$ we find \mathbf{g}^j via

$$\mathbf{g}^j := \operatorname{argsup}_{\mathbf{g} \in \partial J(\mathbf{w})} \mathbf{g}^\top \mathbf{p}^{j-1}. \quad (26)$$

The \mathbf{g}^j given by the above equation are called *violating subgradients* in the sequel. Violating subgradients allow us to recover the true objective $M(\mathbf{p})$ at the iterates \mathbf{p}^{j-1} by noting that

$$M(\mathbf{p}^{j-1}) = M^j(\mathbf{p}^{j-1}) = \frac{1}{2}\mathbf{p}^{j-1\top} \mathbf{B} \mathbf{p}^{j-1} + \mathbf{g}^{j\top} \mathbf{p}^{j-1}. \quad (27)$$

To complete the description what remains to be shown is a procedure to produce the iterates \mathbf{p}^i , which we now elucidate.

We rewrite $\inf_{\mathbf{p} \in \mathbb{R}^d} M^i(\mathbf{p})$ as a constrained optimization problem, which allows us to write the Lagrangian of (25) as

$$L^i(\mathbf{p}, \xi, \alpha) := \frac{1}{2}\mathbf{p}^\top \mathbf{B}^{-1}\mathbf{p} + \xi - \alpha^\top (\xi \mathbf{1} - \mathbf{G}^i \mathbf{p}), \quad (28)$$

7. Note that for ease of exposition we have dropped the iteration index t .

where $\boldsymbol{\alpha} := [\alpha^1; \alpha^2; \dots; \alpha^i]$ is the column vector of non-negative Lagrange multipliers and $\mathbf{G}^i := [\mathbf{g}^1, \mathbf{g}^2, \dots, \mathbf{g}^i] \in \mathbb{R}^{d \times i}$ collects past violating subgradients. Setting the derivative of the Lagrangian w.r.t. the primal variables ξ and \mathbf{p} to 0, respectively, yields

$$\boldsymbol{\alpha}^\top \mathbf{1} = 1 \text{ and} \quad (29)$$

$$\mathbf{p} = -\mathbf{B}\mathbf{G}^i\boldsymbol{\alpha}. \quad (30)$$

The primal variable \mathbf{p} and the dual variable $\boldsymbol{\alpha}$ are related via the dual connection (30). To eliminate the primal variables ξ and \mathbf{p} , we plug (29) and (30) back into the Lagrangian to obtain the dual of $M^i(\mathbf{p})$:

$$\begin{aligned} D^i(\boldsymbol{\alpha}) &:= -\frac{1}{2}(\mathbf{G}^i\boldsymbol{\alpha})^\top \mathbf{B}(\mathbf{G}^i\boldsymbol{\alpha}), \\ \text{s.t. } \boldsymbol{\alpha} &\in [0, 1]^i, \quad \|\boldsymbol{\alpha}\|_1 = 1. \end{aligned} \quad (31)$$

Note that maximizing the dual objective $D^i(\boldsymbol{\alpha})$ (*resp.* minimizing the primal objective $M^i(\mathbf{p})$) can be done exactly via quadratic programming. However, doing so may incur substantial computational expense. Instead we adapt an iterative scheme which is cheap and easy to implement and yet guarantees dual improvement.

Let $\boldsymbol{\alpha}^i \in [0, 1]^i$ be a feasible solution for $D^i(\boldsymbol{\alpha})$.⁸ The corresponding primal solution \mathbf{p}^i can be found by using (30). This in turn allows us to compute the next violating subgradient \mathbf{g}^{i+1} via (26). Given the new violating subgradient we can write the dual $D^{i+1}(\boldsymbol{\alpha})$:

$$\begin{aligned} D^{i+1}(\boldsymbol{\alpha}) &:= -\frac{1}{2}(\mathbf{G}^{i+1}\boldsymbol{\alpha})^\top \mathbf{B}(\mathbf{G}^{i+1}\boldsymbol{\alpha}), \\ \text{s.t. } \boldsymbol{\alpha} &\in [0, 1]^{i+1}, \quad \|\boldsymbol{\alpha}\|_1 = 1, \end{aligned} \quad (32)$$

where the subgradient matrix is now extended:

$$\mathbf{G}^{i+1} = [\mathbf{G}^i, \mathbf{g}^{i+1}]. \quad (33)$$

Our iterative strategy constructs a new feasible solution $\boldsymbol{\alpha} \in [0, 1]^{i+1}$ for $D^{i+1}(\boldsymbol{\alpha})$ by constraining it to take the following form:

$$\boldsymbol{\alpha} := [(1 - \mu)\boldsymbol{\alpha}^i; \mu], \quad \mu \in [0, 1]. \quad (34)$$

In other words we maximize a one-dimensional function $\bar{D}^{i+1} : [0, 1] \rightarrow \mathbb{R}$:

$$\begin{aligned} \bar{D}^{i+1}(\mu) &:= -\frac{1}{2}(\mathbf{G}^{i+1}\boldsymbol{\alpha})^\top \mathbf{B}(\mathbf{G}^{i+1}\boldsymbol{\alpha}) \\ &= -\frac{1}{2}((1 - \mu)\bar{\mathbf{g}}^i + \mu\mathbf{g}^{i+1})^\top \mathbf{B}((1 - \mu)\bar{\mathbf{g}}^i + \mu\mathbf{g}^{i+1}), \end{aligned} \quad (35)$$

where

$$\bar{\mathbf{g}}^i := \mathbf{G}^i\boldsymbol{\alpha}^i \in \partial J(\mathbf{w}) \quad (36)$$

8. Note that $\boldsymbol{\alpha}^1 = [1]$ is a feasible solution for $D^1(\boldsymbol{\alpha})$.

lies in the convex hull of $\mathbf{g}^j \in \partial J(\mathbf{w}) \ \forall j \leq i$ (and hence lies in the convex set $\partial J(\mathbf{w})$) due to $\boldsymbol{\alpha}^i \in [0, 1]^i$ and $\|\boldsymbol{\alpha}^i\|_1 = 1$. Moreover, $\mu \in [0, 1]$ ensures the feasibility of the dual solution. Noting that $\bar{D}^{i+1}(\mu)$ is a concave quadratic function, we set

$$\partial \bar{D}^{i+1}(\mu) = (\bar{\mathbf{g}}^i - \mathbf{g}^{i+1})^\top \mathbf{B} ((1 - \eta)\bar{\mathbf{g}}^i + \eta\mathbf{g}^{i+1}) = 0 \quad (37)$$

to obtain the optimum

$$\mu^* := \operatorname{argmax}_{\mu \in [0, 1]} \bar{D}^{i+1}(\mu) = \min \left(1, \max \left(0, \frac{(\bar{\mathbf{g}}^i - \mathbf{g}^{i+1})^\top \mathbf{B} \bar{\mathbf{g}}^i}{(\bar{\mathbf{g}}^i - \mathbf{g}^{i+1})^\top \mathbf{B} (\bar{\mathbf{g}}^i - \mathbf{g}^{i+1})} \right) \right). \quad (38)$$

Our dual solution at step $i + 1$, then, becomes

$$\boldsymbol{\alpha}^{i+1} := [(1 - \mu^*)\boldsymbol{\alpha}^i; \mu^*]. \quad (39)$$

Furthermore, from (33), (34), and (36) it follows that $\bar{\mathbf{g}}^i$ can be maintained via an incremental update (Step 6 of Algorithm 2):

$$\bar{\mathbf{g}}^{i+1} := \mathbf{G}^{i+1}\boldsymbol{\alpha}^{i+1} = (1 - \mu^*)\bar{\mathbf{g}}^i + \mu^*\mathbf{g}^{i+1},$$

which combined with the dual connection (30) gives an update for the primal solution (Step 7 of Algorithm 2):

$$\mathbf{p}^{i+1} := -\mathbf{B}\bar{\mathbf{g}}^{i+1} = -(1 - \mu^*)\mathbf{B}\bar{\mathbf{g}}^i - \mu^*\mathbf{B}\mathbf{g}^{i+1} = (1 - \mu^*)\mathbf{p}^i - \mu^*\mathbf{B}\bar{\mathbf{g}}^{i+1}. \quad (40)$$

This implies that to derive a primal solution (Step 5–7 of Algorithm 2), it costs a total of $O(d^2)$ time (*resp.* $O(md)$ time for the memory-limited variant with memory buffer size m), d being the dimension of the optimization problem. Note that, in general, maximizing $D^{i+1}(\boldsymbol{\alpha})$ directly via quadratic programming results in a larger progress than that obtained by our approach:

$$0 \leq D^{i+1}(\boldsymbol{\alpha}^{i+1}) - D^{i+1}([\boldsymbol{\alpha}^i; 0]) \leq \max_{\boldsymbol{\alpha} \in [0, 1]^{i+1}, \|\boldsymbol{\alpha}\|_1 = 1} D^{i+1}(\boldsymbol{\alpha}) - D^{i+1}([\boldsymbol{\alpha}^i; 0]).$$

In order to measure the quality of our solution at step i , we define the following quantity:

$$\epsilon^i := \min_{j \leq i} M^{j+1}(\mathbf{p}^j) - D^i(\boldsymbol{\alpha}^i) = \min_{j \leq i} M(\mathbf{p}^j) - D^i(\boldsymbol{\alpha}^i), \quad (41)$$

where the second equality follows directly from (27). Let $D(\boldsymbol{\alpha})$ be the corresponding dual problem of $M(\mathbf{p})$ with the property $D([\boldsymbol{\alpha}^i; 0; \dots; 0]) = D^i(\boldsymbol{\alpha}^i)$; and denote by $\boldsymbol{\alpha}^*$ the optimal solution to $\max_{\boldsymbol{\alpha} \in \mathcal{A}} D(\boldsymbol{\alpha})$, where \mathcal{A} is some domain of interest. Then, the weak duality theorem suggests that $\min_{\mathbf{p} \in \mathbb{R}^d} M(\mathbf{p}) \geq D(\boldsymbol{\alpha}^*)$. Therefore, by the definition of ϵ^i , we get

$$\epsilon^i \geq \min_{\mathbf{p} \in \mathbb{R}^d} M(\mathbf{p}) - D^i(\boldsymbol{\alpha}^i) \geq D(\boldsymbol{\alpha}^*) - D^i(\boldsymbol{\alpha}^i) = D(\boldsymbol{\alpha}^*) - D([\boldsymbol{\alpha}^i; 0; \dots; 0]) \geq 0. \quad (42)$$

This means ϵ^i upper bounds the distance from the optimal dual objective value, $D(\boldsymbol{\alpha}^*)$. In fact, Theorem 3 below shows that $(\epsilon^i - \epsilon^{i+1})$ is bounded away from 0, *i.e.*, ϵ^i is monotonically

decreasing. This guides us to design a practical stopping criteria (Step 4 of Algorithm 2) for our direction-finding procedure. Furthermore, using the dual connection (30), we can derive an implementable formula for ϵ^i :

$$\begin{aligned}\epsilon^i &= \min_{j \leq i} \frac{1}{2} \mathbf{p}^j{}^\top \mathbf{B}^{-1} \mathbf{p}^j + \mathbf{p}^j{}^\top \mathbf{g}^{j+1} + \frac{1}{2} (\mathbf{G}^i \boldsymbol{\alpha}^i)^\top \mathbf{B} (\mathbf{G}^i \boldsymbol{\alpha}^i) \\ &= \min_{j \leq i} -\frac{1}{2} \mathbf{p}^j{}^\top \bar{\mathbf{g}}^j + \mathbf{p}^j{}^\top \mathbf{g}^{j+1} - \frac{1}{2} \mathbf{p}^i{}^\top \bar{\mathbf{g}}^i \\ &= \min_{j \leq i} \mathbf{p}^j{}^\top \mathbf{g}^{j+1} - \frac{1}{2} (\mathbf{p}^j{}^\top \bar{\mathbf{g}}^j + \mathbf{p}^i{}^\top \bar{\mathbf{g}}^i), \\ &\text{where } \mathbf{g}^{j+1} := \operatorname{argsup}_{\mathbf{g} \in \partial J(\mathbf{w})} \mathbf{g}^\top \mathbf{p}^j \text{ and } \bar{\mathbf{g}}^j := \mathbf{G}^j \boldsymbol{\alpha}^j \quad \forall j \leq i.\end{aligned}$$

It is worth noting that continuous progress in the dual objective value does not necessarily prevent an increase in the primal objective value, *i.e.*, it is possible that $M(\mathbf{p}^{i+1}) \geq M(\mathbf{p}^i)$. Therefore, we choose the best so far primal solution, $\mathbf{p} := \operatorname{argmin}_{j \leq i} M(\mathbf{p}^j)$, as the search direction (Step 15 of Algorithm 2) for the parameter update (3). It is easy to check that if \mathbf{p}^i fulfills the descent condition (9), then so does \mathbf{p} .

In what follows, we prove the convergence of Algorithm 2 via several technical intermediate steps.

Lemma 1 *Denote by $\bar{D}^{i+1}(\mu)$ the one-dimensional function defined in (35) and ϵ^i the positive measure defined in (41). Then,*

$$\epsilon^i \leq \partial \bar{D}^{i+1}(0). \quad (43)$$

Proof Let \mathbf{p}^i be our primal solution at step i , derived from the dual solution $\boldsymbol{\alpha}^i$ using the dual connection (30). Then, we have

$$\mathbf{p}^i = -\mathbf{B} \bar{\mathbf{g}}^i, \text{ where } \bar{\mathbf{g}}^i := \mathbf{G}^i \boldsymbol{\alpha}^i. \quad (44)$$

It follows from the definition of $M(\mathbf{p})$ (24) that

$$M(\mathbf{p}^i) = \frac{1}{2} \mathbf{p}^i{}^\top \mathbf{B}^{-1} \mathbf{p}^i + \mathbf{p}^i{}^\top \mathbf{g}^{i+1},$$

where

$$\mathbf{g}^{i+1} := \operatorname{argsup}_{\mathbf{g} \in \partial J(\mathbf{w})} \mathbf{g}^\top \mathbf{p}^i. \quad (45)$$

Using (44), we have $\mathbf{B}^{-1} \mathbf{p}^i = -\mathbf{B}^{-1} \mathbf{B} \bar{\mathbf{g}}^i = -\bar{\mathbf{g}}^i$, which implies

$$M(\mathbf{p}^i) = \mathbf{p}^i{}^\top \mathbf{g}^{i+1} - \frac{1}{2} \mathbf{p}^i{}^\top \bar{\mathbf{g}}^i. \quad (46)$$

Similarly, we have

$$D^i(\boldsymbol{\alpha}^i) = -\frac{1}{2} (\mathbf{G}^i \boldsymbol{\alpha}^i)^\top \mathbf{B} (\mathbf{G}^i \boldsymbol{\alpha}^i) = \frac{1}{2} \mathbf{p}^i{}^\top \bar{\mathbf{g}}^i. \quad (47)$$

From (37) and (44) it follows that

$$\partial \bar{D}^{i+1}(0) = (\bar{\mathbf{g}}^i - \mathbf{g}^{i+1})^\top \mathbf{B} \bar{\mathbf{g}}^i = (\mathbf{g}^{i+1} - \bar{\mathbf{g}}^i)^\top \mathbf{p}^i, \quad (48)$$

where \mathbf{g}^{i+1} is a violating subgradient chosen via (26), and hence coincides with (45). Using (46), (47) and (48), we get

$$M(\mathbf{p}^i) - D^i(\boldsymbol{\alpha}^i) = (\mathbf{g}^{i+1} - \bar{\mathbf{g}}^i)^\top \mathbf{p}^i = \partial \bar{D}^{i+1}(0),$$

from which and the definition of ϵ^i , it follows

$$\epsilon^i = \min_{j \leq i} M(\mathbf{p}^j) - D^i(\boldsymbol{\alpha}^i) \leq M(\mathbf{p}^i) - D^i(\boldsymbol{\alpha}^i) = \partial \bar{D}^{i+1}(0)$$

■

Lemma 2 Denote by $f : [0, 1] \rightarrow \mathbb{R}$ a concave quadratic function with $f(0) = 0$, $\partial f(0) \in [0, h]$, and $\partial f^2(x) \geq -h$ for some $h \geq 0$. Then, for all $x \in [0, 1]$ we have $\max_{x \in [0, 1]} f(x) \geq \frac{(\partial f(0))^2}{2h}$.

Proof Using a second-order Taylor expansion around 0, we have $f(x) \geq \partial f(0)x - \frac{h}{2}x^2$. $x^* = \partial f(0)/h$ is the unconstrained maximum of the lower bound. Since $\partial f(0) \in [0, h]$, we have $x^* \in [0, 1]$. Plugging x^* into the lower bound yields $(\partial f(0))^2/(2h)$. ■

Theorem 3 Assume that at \mathbf{w} the convex objective function $J : \mathbb{R}^d \rightarrow \mathbb{R}$ has bounded subgradient, i.e., $\|\partial J(\mathbf{w})\| \leq G$. Also assume that approximation \mathbf{B} to the inverse Hessian is bounded, i.e., $\|\mathbf{B}\| \leq H$. Then,

$$\epsilon^i - \epsilon^{i+1} \geq \frac{(\epsilon^i)^2}{8G^2H}. \quad (49)$$

Proof Recall that we constrain the form of feasible dual solutions for $D^{i+1}(\boldsymbol{\alpha})$ to $[(1 - \mu)\boldsymbol{\alpha}^i; \mu]$, where $\boldsymbol{\alpha}^i \in [0, 1]^i$ and $\|\boldsymbol{\alpha}^i\|_1 = 1$. Thus, instead of $D^{i+1}(\boldsymbol{\alpha})$, we work with the one-dimensional concave quadratic function of μ : $\bar{D}^{i+1} : [0, 1] \rightarrow \mathbb{R}$ (35) with $\bar{D}^{i+1}(\mu) = D^{i+1}([(1 - \mu)\boldsymbol{\alpha}^i; \mu])$. It is obvious that $[\boldsymbol{\alpha}^i; 0]$ is a feasible solution for $D^{i+1}(\boldsymbol{\alpha})$. In this case, $\bar{D}^{i+1}(0) = D^i(\boldsymbol{\alpha}^i)$. It follows from (39) that $\bar{D}^{i+1}(\mu^*) = D^{i+1}(\boldsymbol{\alpha}^{i+1})$. Therefore, using the definition of ϵ^i (41), we have

$$\epsilon^i - \epsilon^{i+1} \geq D^{i+1}(\boldsymbol{\alpha}^{i+1}) - D^i(\boldsymbol{\alpha}^i) = \bar{D}^{i+1}(\mu^*) - \bar{D}^{i+1}(0).$$

It is easy to see that $(\epsilon^i - \epsilon^{i+1})$ upper bounds the maximal value of the concave quadratic function: $f(\mu) := \bar{D}^{i+1}(\mu) - \bar{D}^{i+1}(0)$ with $\mu \in [0, 1]$ and $f(0) = 0$. Furthermore, from the definitions of $\bar{D}^{i+1}(\mu)$ and $f(\mu)$ it follows that

$$\begin{aligned} \partial f(0) &= \partial \bar{D}^{i+1}(0) = (\bar{\mathbf{g}}^i - \mathbf{g}^{i+1})^\top \mathbf{B} \bar{\mathbf{g}}^i \text{ and} \\ \partial^2 f(\mu) &= \partial^2 \bar{D}^{i+1}(\mu) = -(\bar{\mathbf{g}}^i - \mathbf{g}^{i+1})^\top \mathbf{B} (\bar{\mathbf{g}}^i - \mathbf{g}^{i+1}). \end{aligned} \quad (50)$$

Since $\|\partial J(\mathbf{w})\| \leq G$ and $\bar{\mathbf{g}}^i \in \partial J(\mathbf{w})$ (36), we have $\|\bar{\mathbf{g}}^i - \mathbf{g}^{i+1}\| \leq 2G$. Our assumption on $\|\mathbf{B}\|$, then, gives $|\partial f(0)| \leq 2G^2H$ and $|\partial^2 f(\mu)| \leq 4G^2H$. Additionally, inequality (43) and the fact that $\mathbf{B} \succ 0$ imply

$$\partial f(0) = \partial \bar{D}^{i+1}(0) \geq 0 \quad \text{and} \quad \partial^2 f(\mu) = \partial^2 \bar{D}^{i+1}(\mu) < 0, \quad (51)$$

which means

$$\partial f(0) \in [0, 2G^2H] \subset [0, 4G^2H] \quad \text{and} \quad \partial^2 f(\mu) > -4G^2H. \quad (52)$$

Invoking Lemma 2, we immediately get

$$\epsilon^i - \epsilon^{i+1} \geq \frac{(\partial f(0))^2}{8G^2H} = \frac{(\partial \bar{D}^{i+1}(0))^2}{8G^2H}. \quad (53)$$

Since $\epsilon^i \leq \partial \bar{D}^{i+1}(0)$ by Lemma 1, the inequality in (53) still holds when $\partial \bar{D}^{i+1}(0)$ is substituted with ϵ^i . \blacksquare

Note that (50) and (51) imply that the optimal combination coefficient μ^* (38) has the following property:

$$\mu^* = \min \left(1, \frac{\partial \bar{D}^{i+1}(0)}{-\partial^2 \bar{D}^{i+1}(\mu)} \right). \quad (54)$$

Moreover, using (30), we set $\mathbf{B}\bar{\mathbf{g}}^i$ in (38) to be \mathbf{p}^i (Step 5 of Algorithm 2) to reduce the cost of computing μ^* .

The following technical lemma is given as Sublemma 5.4 and proven by induction in (Abe et al., 2001).

Lemma 4 *Let $\{\epsilon^1, \epsilon^2, \dots, \epsilon^i\}$ $i \in \mathbb{N}$ be a sequence of non-negative numbers satisfying the following recurrence:*

$$\epsilon^i - \epsilon^{i+1} \geq c (\epsilon^i)^2,$$

where $c \in \mathbb{R}_+$ is a positive constant. Then, for all $i \geq 1$, we have

$$\epsilon^i \leq \frac{1}{c \left(t + \frac{1}{\epsilon^1 c} \right)}.$$

We are now ready to show in Theorem 5 that Algorithm 2 decreases ϵ^i to a pre-defined tolerance ϵ in $O(1/\epsilon)$ steps.

Theorem 5 *Under the assumptions of Theorem 3 Algorithm 2 converges to the desired precision ϵ after*

$$n \leq \frac{8G^2H}{\epsilon} - 4$$

steps for any $\epsilon < 2G^2H$.

Proof It follows from Theorem 3 that

$$\epsilon^i - \epsilon^{i+1} \geq \frac{(\epsilon^i)^2}{8G^2H},$$

where $\epsilon^i \forall i \in \mathbb{N}$ is non-negative by (42). Thus, applying Lemma 4, we get

$$\epsilon^i \leq \frac{1}{c \left(t + \frac{1}{\epsilon^1 c}\right)}, \quad \text{where } c := \frac{1}{8G^2H}. \quad (55)$$

Our assumptions on $\|\partial J(\mathbf{w})\|$ and $\|\mathbf{B}\|$ imply $\bar{D}^{i+1}(0) = (\bar{\mathbf{g}}^i - \mathbf{g}^{i+1})^\top \mathbf{B} \bar{\mathbf{g}}^i \leq 2G^2H$. Hence, $\epsilon^i \leq 2G^2H$ by Lemma 1. This means the inequality (55) holds with $\epsilon^1 = 2G^2H$. Therefore, we can solve the following equation

$$\epsilon = \frac{1}{c \left(t + \frac{1}{\epsilon^1 c}\right)}, \quad \text{with } c := \frac{1}{8G^2H} \text{ and } \epsilon^1 := 2G^2H, \quad (56)$$

to obtain an upper bound t on the number of steps n such that $\epsilon^n < \epsilon < 2G^2H$. The solution to (56) is $t = \frac{8G^2H}{\epsilon} - 4$. Hence, we prove our claim. \blacksquare

Appendix B. Positive Step Size

To formally show that there exists a positive step size satisfying the subgradient Wolfe conditions (14), we need Theorem 2.3.3 of Hiriart-Urruty and Lemaréchal (1993), which we restate in a slightly modified form:

Lemma 6 *Given two points $\mathbf{w} \neq \mathbf{w}'$ in \mathbb{R}^d define $\mathbf{w}_\eta = \eta \mathbf{w}' + (1 - \eta) \mathbf{w}$. Let $J : \mathbb{R}^d \rightarrow \mathbb{R}$ be convex. There exists $\eta \in (0, 1)$ such that*

$$J(\mathbf{w}') - J(\mathbf{w}) \leq \sup_{\mathbf{g} \in \partial J(\mathbf{w}_\eta)} \mathbf{g}^\top (\mathbf{w}' - \mathbf{w}). \quad (57)$$

Theorem 7 *Suppose $\Phi(\eta) := J(\mathbf{w} + \eta \mathbf{p}) \forall \eta > 0$ is lower bounded. Let \mathbf{p} be a descent direction at an iterate \mathbf{w} . Then, there exists a positive step size η satisfying the subgradient Wolfe conditions (14).*

Proof Since \mathbf{p} is a descent direction, the line $J(\mathbf{w}) + c_1 \eta \sup_{\mathbf{g} \in \partial J(\mathbf{w})} \mathbf{g}^\top \mathbf{p}$ with $c_1 \in (0, 1)$ must intersect $\Phi(\eta)$ at least once at some $\eta > 0$ (see Figure 3 for geometric intuition). Let η' be the smallest such intersection point; then,

$$J(\mathbf{w} + \eta' \mathbf{p}) = J(\mathbf{w}) + c_1 \eta' \sup_{\mathbf{g} \in \partial J(\mathbf{w})} \mathbf{g}^\top \mathbf{p}. \quad (58)$$

Since $\Phi(\eta)$ is lower bounded, the first condition in (14) holds for all $\eta'' \in [0, \eta']$.

Setting $\mathbf{w}' = \mathbf{w} + \eta' \mathbf{p}$ in lemma 6, it follows that there exists $\eta'' \in (0, \eta')$ such that

$$J(\mathbf{w} + \eta' \mathbf{p}) - J(\mathbf{w}) \leq \eta' \sup_{\mathbf{g} \in \partial J(\mathbf{w} + \eta'' \mathbf{p})} \mathbf{g}^\top \mathbf{p}. \quad (59)$$

Plugging in (58) and simplifying yields

$$c_1 \sup_{\mathbf{g} \in \partial J(\mathbf{w})} \mathbf{g}^\top \mathbf{p} \leq \sup_{\mathbf{g} \in \partial J(\mathbf{w} + \eta'' \mathbf{p})} \mathbf{g}^\top \mathbf{p}. \quad (60)$$

Since \mathbf{p} is a descent direction it follows that $\sup_{\mathbf{g} \in \partial J(\mathbf{w})} \mathbf{g}^\top \mathbf{p} < 0$, and hence the above inequality also holds when c_1 is replaced by $c_2 \in (c_1, 1)$. ■